DESIGN AND OPTIMIZATION OF FUTURE X-RAY FELS BASED ON ADVANCED HIGH FREQUENCY LINACS*

Faya Wang#, SLAC National Accelerator Laboratory, Menlo Park, CA 94025, U.S.A.

Abstract

To drive future XFELs, normal-conducting linacs at various rf freqencies are being considered. With optimized accelerator structures and rf systems, a higher rf frequency linac has several advantages, such as high acceleration gradient and high rf-to-beam efficiency. This paper presents a comparison of possible S-band, C-band and X-band linac designs for two cases, single bunch operation and multibunch operation, where the bunch train length is longer than the structure fill time and the beam loading is small. General scaling laws for the main linac parameters, which can be useful in the design such linacs, are derived.

INTRODUCTION

With the successful operation of the first hard X-ray FEL, LCLS, other XFEL facilities are being developed worldwide. Those driven by normal-conducting linacs fall into two main groups. The first uses S-band linacs, including LCLS at SLAC [1], XFEL at PAL [2], SPARX-FEL [3] and MAX IV [4]; the second uses C-band developed for the SCSS XFEL [5], including SwissFEL at PSI [6] and Shanghai XFEL [7]. Switching from S-band to C-band enables a higher acceleration gradient (35 MV/m) that is nearly double that of the SLAC S-band Linac. This is a major consideration for the Shanghai XFEL, as they are limited by the available site size. SPARX-FEL and XFEL at PAL are considering C-band technology for higher gradient linac extensions.

Still higher gradients are possible at X-band: 65 MV/m and higher was achieved in prototype NLC structures [8], and 100 MV/m has been achieved in structures being developed for CLIC [9]. A SLAC-LLNL collaboration is currently using the NLC X-band technology to build a compact Compton gamma ray source [10].

In spite of the strong increase in wakefield strength with rf frequency, the very short, low-charge bunches required for XFELs, along with the shorter linac length afforded by the higher acceleration gradient, can make high frequency linacs a viable choice. Opting for a higher frequency reduces significantly the rf energy required at a given gradient. In this paper, we compare design parameters of linacs at S-band (2.856 GHz), C-band (5.712 GHz) and X-band (11.424 GHz), denoting them by S, C and X, respectively.

THE RF POWER TO BEAM CONVERSION EFFICIENCY

The rf to beam conversion efficiency, η, is directly related to the choice of the rf frequency, which has a strong influence on the overall facility complexity and cost. For very low beam loading, normal conducting, constant gradient, travelling wave (CG-TW) accelerators powered by a square rf pulse, the efficiency is given by,

$$\eta = \frac{rI_bT_b}{G}\left(1-e^{-2\tau}\right)\Big/\left(T_b+2\tau Q/\omega\right), \quad (1)$$

where r, τ, Q, G, ω, I_b, and T_b are, respectively, the structure shunt impedance per unit length, field attenuation constant, unloaded Q, gradient, rf frequency, beam current and beam macro pulse (bunch train) length.

For a given value of T_b, maximum rf to beam efficiency is obtained when

$$e^{2\tau_{opt}} - 2\tau_{opt} = T_b\omega/Q + 1, \quad (2)$$

The optimal field attenuation constant, τ_{opt}, can be approximated by,

$$\tau_{opt} \approx \begin{cases} \sqrt{\dfrac{T_b\omega}{2Q}}, & \text{(a)} \\ \dfrac{1}{2}\log\left(\dfrac{T_b\omega}{Q}+1\right), & \text{(b)} \end{cases} \quad (3)$$

where (a) and (b) are, respectively, for the cases of very short beam pulse length ($T_b << T_f$, where T_f is the filling time of the structure), e.g. single/double bunches, and very long beam pulse length ($T_b >> T_f$). Fig.1 shows the optimum field attenuation constant versus the beam pulse length for the three rf frequencies being considered.

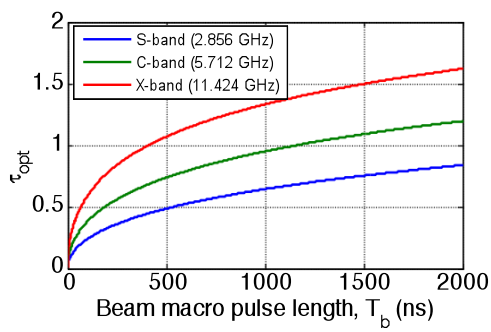

Figure 1: Optimum field attenuation versus beam pulse length with Q assumed proportional to $\omega^{-1/2}$ and taken as 13,400 for S-band.

LINAC DESIGN FOR A SHORT BEAM PULSE

Accelerator Structure Design

We first consider two-bunch operation where the bunches are spaced by 50 ns. We also assume 1) CG-TW structures with 2π/3 phase advance, 2) a constant value for the average iris radius to rf wavelength ratio (a/λ) and

* Work supported by the U.S. Department of Energy under contract DE-AC02-76SF00515.
# fywang@slac.stanford.edu

3) that the average Q and shunt impedance are proportional, respectively, to $\omega^{-1/2}$ and $\omega^{1/2}$ and are 13,400 and 60 MΩ/m for S-band. Fig. 2 shows the relative rf power to beam conversion efficiency for S, C and X linacs as a function of the structure field attenuation constant for gradients of 20 MV/m, 40 MV/m and 80 MV/m, respectively. It clearly illustrates the key advantage of high frequency linacs in that the maximum efficiency is nearly proportional to $\omega^{1/2}$ even when the gradient increases in proportion to ω. In addition, the plot shows the efficiencies for existing S, C and X structures. These latter structures were optimized for higher beam loading and are not optimal for the case considered here.

The above comparison assumes a constant a/λ, whereas one can use smaller values at lower frequency due to the smaller wakes. This will increase the shunt impedance and efficiency at lower frequencies. How one chooses to do this depends on the goal, and we consider three different options: S1 produces the smallest value of a/λ to obtain the highest shunt impedance, S2 produces realistic structure lengths and S3 scales the structure length with rf wavelength to reduce the cost of rf feeds. For comparison of these designs, the X-band structure is assumed to have an average iris size of 4 mm for all three cases. However, in this case, option S1 would have a very small average a/λ (< 0.08) and a structure length less than 0.3 m for S and C. As this is not realistic for TW structures, standing wave structures (SW) are assumed for S and C for S1, with iris sizes that produce the same relative transverse wakefield effect on the bunches as in X. Also, the coupling for each SW structure is chosen to minimize the rf energy required. With these choices, the optimum structure parameters for the three design options are listed in Table 1.

X still requires the least amount of rf energy, even with these more optimal S and C choices. Also, the higher the shunt impedances in the S and C cases for S1 lowers the structure stored energy, but the longer filling time lowers efficiency, and about 50% more rf energy is needed compared to the TW designs.

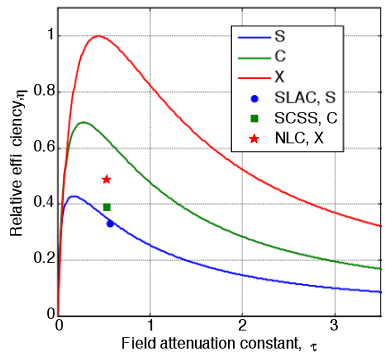

Figure 2: Relative rf power to beam conversion efficiency for S, C and X-band linacs for 50 ns beam pulses as functions of the structure field attenuation constant.

High Power RF System

To make these cases more realistic, we now factor in the effect of using existing klystrons to power the structures. While the available klystron pulse width is few microseconds for S, C and X, the required rf pulse width for short beam applications is only a few hundred nanoseconds. To reduce capital cost, we assume a SLED pulse compression system [11] is used to boost the rf peak power, which is then used to feed multiple structures. The parameters of the resulting rf units are listed in Table 2, which again shows X-band requires less rf energy despite the much higher gradient.

Table 1: Optimum structure parameters for the three different options with a 50 ns beam pulse width (T_b). The rf to beam energy ratio is defined as $U_{rf}/\Delta U_b$, where $U_{rf} = P_{rf}(T_f + T_b)$ and ΔU_b is the beam energy increase per electron.

RF Frequency		**S**			**C**		**X**	**Unit**
Design Option	S1	S2	S3	S1	S2	S3		
Length	105	63	241.6	52.5	63	120.8	60.4	cm
Number of Cells	20	18	69	20	36	69	69	
Filling Time, T_f	549	269	265	299	151	150	77	ns
Phase Advance	180	120	120	180	120	120	120	°/cell
Q ($\sim \omega^{-1/2}$)	17,600	13,887	13,887	12,190	9,419	9,419	6,231	
Field Attenuation, τ	-	0.17	0.17	-	0.29	0.29	0.44	
Group Velocity, v_g/c	-	0.93–0.67	3.54–2.51	-	1.83–1.05	3.49–1.98	3.93–1.65	%
Norm. Iris Size, $\langle a/\lambda \rangle$	5.2	9.5	13.2	9.0	12.0	13.9	15.2	%
Iris Size, a	5.5	10.39–9.62	14.46–13.24	4.7	6.68–5.90	7.78–6.82	4.37–3.62	mm
Iris Thickness, t ($\sim \omega^{-1/2}$)		5			3.5		2.5	mm
Shunt Impedance, r_s	62	68–70	56–60	78	79–85	70–78	78–95	MΩ/m
SW Coupling	4.83	-	-	3.21	-	-	-	
Gradient		20			40		80	MV/m
Peak rf Power Needed	18.4	12.6	56.9	21.2	28.4	60.1	77.1	MW
RF to beam energy ratio	**0.53**	**0.32**	**0.38**	**0.34**	**0.23**	**0.25**	**0.20**	**J/MeV**

Table 2: RF units for 50 ns beam pulse operation for the various structure options.

RF Freq.	**S**			**C**			**X**	**Unit**
Klystron Type	5045			E3747			XL-4	
Number of Klystrons	1			1			2	
Modulator HV	350			350			400	kV
Klystron Peak Power	65			50			50	MW
Max. Klystron Pulse Width	3.5			2.5			1.5	
Accelerator Designs	S1	S2	S3	S1	S2	S3		
Required Klystron Pulse Width	3.5	1.5	1.5	2.5	1	1	0.6	μs
SLED Compression Ratio	5.83	5.1		7.14	5.6		5.6	
SLED Cavity Mode	$TE_{0,1,5}$ [11]			$TE_{0,1,15}$ [12]			$TE_{0,1,10}$ [13]	
SLED Cavity Length	33.59			43.27			13.56	cm
SLED Cavity Diameter	20.51			15.26			12.25	cm
SLED Cavity	1.08×10^5			1.81×10^5			1.09×10^5	
SLED Cavity Beta	6.55	16.8		8.19	22.8		12.4	
Power Gain of SLED	2.77	3.61		3.25	3.61		3.61	
Efficiency of SLED	47.5	71		45.5	65		64	%
Number of Accelerators	10	19	4	8	6	3	5	
Linac Length	10.5	12	9.7	4.2	3.8	3.6	3.0	m
Acceleration Gradient	19.8	19.8	20.3	39.1	41.2	40	77.4	MV/m
Beam Energy	208	237	196	165	156	145	234	MeV
Klystron rf to beam energy ratio	**1.1**	**0.41**	**0.5**	**0.77**	**0.32**	**0.34**	**0.26**	**J/MeV**

LINAC DESIGN FOR A LONG BEAM PULSE

For an XFEL operated with a multibunch train, the optimal accelerator parameters are quite different from those for single bunch operation, as the optimum field attenuation varies with beam pulse width, as shown in Eq. (2).

For the requirement of a very long beam pulse (close to the klystron pulse width), we assume the X-band operating gradient is reduced to 50 MV/m in order to a) reduce the peak power required as SLED is no longer practical and b) achieve a manageable rf breakdown rate. According to empirically derived scaling laws [12], the acceleration gradient for a fixed breakdown rate is reduced 30% when the rf pulse width is increased by a factor of eight. At an rf pulse width of 1.5 μs for the X-band NLC structure (T53VG3), which is the pulse length rating for the 50 MW XL4 klyston, the predicted breakdown rate is about 0.025/hr at a repetition rate of 120 Hz, which is low enough for an XFEL. For a beam pulse width of 1.25 μs, Fig. 3 shows the relative rf power to beam conversion efficiency for S, C and X linacs as functions of the accelerator structure field attenuation constant where the same phase advance, Q and shunt impedance assumptions were made as for the short pulse case described above. The acceleration gradients are, respectively, 20 MV/m, 40 MV/m, and 50 MV/m. In this case, the S and C structures would need to operate reliably at pulse widths several times that currently demostrated at these gradients, which may not be possible.

Based on fabrication experience, cost and amount of rf power required, the length chosen for an X-band structure typically does not exceed a meter. The value of τ_{opt}, from Fig.3, is 1.4 for X-band. For a 1 meter, X-band, $2\pi/3$, CG-TW structure with this field attenuation, the iris radius for the last cell of the structure is about 2.5 mm, which would generate very strong wakefields.

For a fixed value of τ, the length of a $2\pi/3$, CG-TW accelerator structure varies with the average iris size $\langle a/\lambda \rangle$ as shown in Fig.4. Reducing τ from the optimum of 1.4 to 0.9 for a 1 m, X-band structure, we can reduce the strength of the transverse wakefield by 50% due to the increased iris size, at a cost of only 10% in rf power to beam energy conversion efficiency.

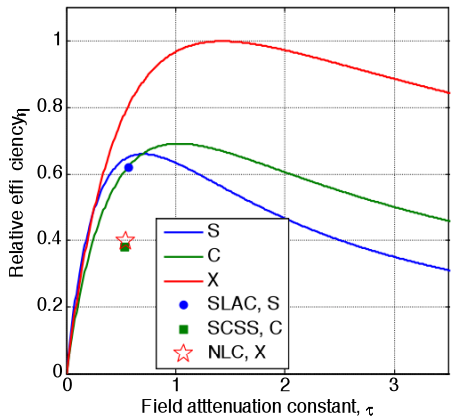

Figure 3: Relative rf power to beam conversion efficiency for S, C and X-band linacs as functions of structure field attenuation constant for 1.25 μs beam pulses.

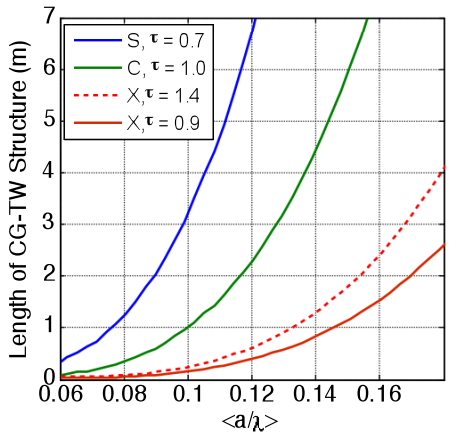

Figure 4: Length of 2π/3, CG-TW structures for S, C and X as functions of average iris size ⟨a/λ⟩ at the given fixed values of field attenuation.

Table 3: Optimized structure parameters for the two options for a 1250 ns beam pulse width.

RF Frequency	**S**		**C**		**X**	**Unit**
Design Option	L1	L2	L1	L2		
Length	105	402.7	94.5	201.3	99.8	cm
Number of Cells	30	115	54	115	114	
Filling Time, T_f	1043	999	514	511	159	ns
Q (~ $\omega^{-1/2}$)	13,887	13,887	9,420	9,420	6,231	
Field Attenuation, τ	0.67	0.65	0.98	0.97	0.92	
Group Velocity, v_g/c	0.6–0.17	2.38–0.67	1.39–0.21	2.97–0.44	4.54–0.74	%
Norm. Iris Size, ⟨a/λ⟩	7.8	10.8	9.0	11.8	14.5	%
Iris Size, a	9.38–7.0	13.07–9.59	6.28–5.45	7.48–4.87	4.52–3.08	mm
Iris Thickness, t (~ $\omega^{-1/2}$)	5		3.5		2.5	mm
Shunt Impedance, r_s	71–76	60–70	82–97	72–93	75–107	MΩ/m
Gradient	20		40		50	MV/m
Peak rf power needed, P_{rf}	7.8	34.3	19.9	46.5	33.7	MW
RF to beam energy ratio	**0.85**	**0.852**	**0.93**	**0.928**	**0.95**	**J/MeV**

As in the short beam case, we now look at changing a/λ to improve the S and C efficiency. In this long beam case, two options are considered: L1 assumes a 1 meter structure length for S, C and X and L2) assumes the structure length is proportional to the rf wavelength. The X-band structure parameters are fixed with an average iris radius of 3.8 mm for the two cases. Table 3 shows the resulting optimized structure parameters for S, C and X. In this case, the rf required for X is somewhat higher than in S and C, but the X gradient is larger.

SUMMARY

For normal-conducting linacs in the cases of a short beam pulse width (50 ns) and a long beam pulse width (1.25 μs) with small beam loading, optimized accelerator structures were presented for three rf technologies: S-band, C-band and X-band. Also, possible rf systems using SLED are described in the short beam case where SLED is applicable. Instead of the general square root of frequency dependence of shunt impedance that occurs with constant ⟨a//λ⟩, the shunt impedance of more realistic structures is proportional to $\omega^{1/6}$ as derived from the results in Tables 1 and 3. This is because ⟨a/λ⟩ needs to 1) be larger to reduce the stronger wakefield at higher rf frequency and 2) be adjusted to obtain a realistic structure length. With the assumptions of low beam loading, CG-TW structures and the $\omega^{1/6}$ shunt impedance scaling, other scaling laws that result are listed in Table 4 for short and long beam pulses. A comparison of results for the relative rf energy per unit beam energy is shown in Figs. 5 and 6, respectively, for 50 ns and 1.25 μs beam pulses. They show that the derived efficiency scaling laws do well to characterize our optimized designs.

Table 4: Realistic scaling laws for a CG-TW linac with low beam loading, where G is the acceleration gradient.

	Short beam pulse, $T_b << T_f$	**Long beam pulse, $T_b >> T_f$**
Shunt Impedance, r_s	$\sim \omega^{1/6}$	$\sim \omega^{1/6}$
Fundamental Mode, Q	$\sim \omega^{-1/2}$	$\sim \omega^{-1/2}$
Field Attenuation Constant, τ	$\sim \omega^{3/4}$	$\sim \omega^{1/2}$
Filling Time, T_f	$\sim \omega^{-3/4}$	$\sim \omega^{-1}$
RF Power per unit Length, P_{rf}/L	$\sim G^2\omega^{-11/12}$	$\sim G^2\omega^{-1/6}$
RF Power to Beam Efficiency, η	$\sim G^{-1}\omega^{5/3}$	$\sim G^{-1}\omega^{2/3}$
Repetition Rate*	$\sim G^{-2}\omega^{-4/3}$	$\sim G^{-2}\omega^{-11/6}$

* assuming constant cooling rate per unit surface area.

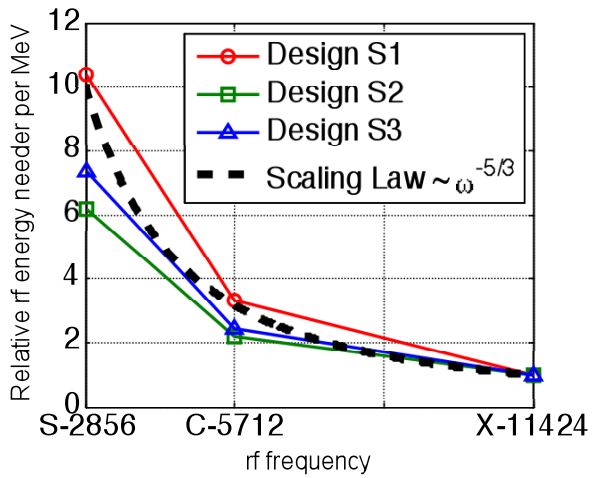

Figure 5: The relative rf energy needed per MeV beam for S, C and X with different optimum designs for a 50 ns beam pulse width.

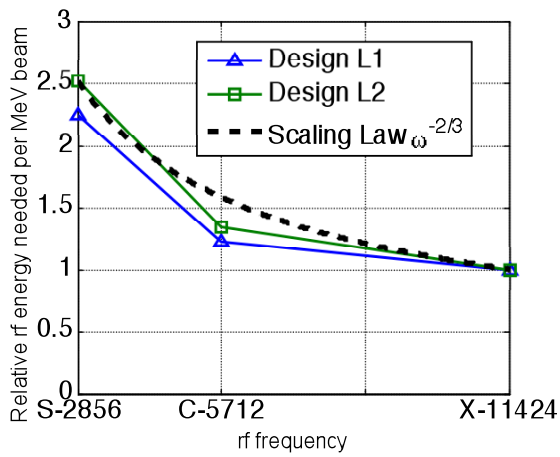

Figure 6: The relative rf energy needed per MeV beam for S, C and X with different optimum designs for a 1250 ns beam pulse width.

REFERENCES

[1] Arthur, J. Materlik, G. Tatchyn, R. Winick, The LCLS: A fourth generation light source using the SLAC linac, RSI, Vol. 66 (2), Feb, 1995.

[2] H.-S. Kang, PAL XFEL, EFST workshop on Compact X-ray Free-Electron Lasers (2010).

[3] L. Palumbo *et al.*, SPARX-FEL Technical Design Report V2.0, 2009, http://www.sparx-fel.it.

[4] M. Eriksson *et al.*, MAX IV, Conceptual Design Report, http://www.maxlab.lu.se/maxlab/max4/index.html.

[5] T. Shintake, Soft X-Ray SASE-FEL Project as Spring-8 Japan, Proc. APAC2001, 2001.

[6] R. Ganter *et al.*, SwissFEL conceptual design report, PSI report 10-04(2010). http://www.psi.ch/swissfel.

[7] C. Feng, Design Studies of Shanghai Hard XFEL, EFST workshop on Compact X-ray Free-Electron Lasers(2010), http://www.sinap.ac.cn/compactxfel10.

[8] Chris Adolphsen, "Advances in Normal Conducting Accelerator Technology from the X-Band Linear Collider Program," SLAC-PUB-11224, June 2005.

[9] C. Adolphsen *et al.*, "Results from the CLIC X-Band Structure Test Program at NLCTA," SLAC-PUB-13697, July 6, 2009.

[10] F. Hartemann *et al.*, "Velociraptor: LLNL's Precision Compton Scattering Light Source," proc. FEL2010, Malmo, Sweden.

[11] Z.D. Farkas, H.A. Hogg, G.A. Loew and P.B. Wilson, SLAC-PUB-1453, 1974.

[12] T. Shintake, N. Akasaka and H. Matsumoto, "Development of C-band RF Pulse Compression System for e^+e^- Linear Collider", PAC09.

[13] Private communication with Christopher D. Nantista.

[14] A. Grudiev, S. Calatroni, W. Wuensch, Physical Review Special Topics – Accelerators and Beams 12, 102001 (2009).